A computational study of brightness-related responses in visual cortex

Bo Cao

Program in Cognitive and Neural Systems, Boston University, Boston, MA, USA

Ennio Mingolla

Department of Speech, Language, Pathology, and Audiology, Northeastern University, Boston, MA, USA

Arash Yazdanbahksh

Center for Computational Neuroscience and Neural Technology, Program in Cognitive and Neural Systems, Boston University, Boston, MA, USA

Rossi, Rittenhouse, and Paradiso (1996) reported a cut-off at 4 Hz in the modulation amplitude of neural responses to large (up to 14°) simultaneous contrast stimuli in the striate cortex of cats, as the temporal frequency of the luminance of flanking patches increased, while the luminance of a central patch covering the neurons' classical receptive fields (CRFs) was held constant. This indicates that the modulation may involve slow processing of information in visual cortex. We develop models with a small set of parameters to explain these brightness-related responses in visual cortex. A model with any of the following mechanisms can fit the data: (a) slow local inhibition (Slow Inhibition Model); (b) slow excitation of the nodes in the second of two layers, which feed back to the inhibitory nodes in the first layer (Slow Excitation Model); and (c) conduction delays along lateral connections (Delay Model). However, the Slow Inhibition Model predicts that neurons in extrastriate cortex show similar response modulations as neurons in V1, while the Slow Excitation Model predicts that, unlike the modulations of V1 neurons shown in the experimental data, neurons in extrastriate cortex show slow modulations of responses to both the direct luminance change and the simultaneous contrast stimuli. The Delay Model predicts that the cut-off frequency of the response modulations depends on the distance from the flanker to the CRFs of the neurons. Further physiological experiments could clarify which mechanism plays an important role in the brightness-related responses in visual cortex.

Keywords: brightness, simultaneous contrast, visual cortex, computational modeling

Citation: Cao, B., Mingolla, E., & Yazdanbahksh, A. (2013). A computational study of brightness-related responses in visual cortex. *Journal of Vision*, *13*(1):8, 1–15, http://www.journalofvision.org/content/13/1/8, doi:10.1167/13.1.8.

Introduction

Many studies have reported that brightness information can be encoded in the primary visual cortex or V1 (Rossi, Rittenhouse, & Paradiso, 1996; Rossi & Paradiso, 1999; Kinoshita & Komatsu, 2001; Friedman, Zhou, & von der Heydt, 2003; Roe, Lu, & Hung, 2005). Some V1 neurons show response fluctuations that track the temporal profile of luminance change of surrounding areas that are several degrees away from the cells' receptive fields, while the luminance of the area that covers the receptive fields stays constant (Rossi et al., 1996; Rossi & Paradiso, 1999). These studies used a central luminance patch (usually 14° × 14° in visual angle) flanked by two other luminance patches to cover the receptive field of the probed V1 neurons (usually less than 5° in height and width; see Figure 1). Thus, the flanking parts are well outside the borders of the classical receptive fields (CRF) of the neurons. Two typical experimental conditions are: (a) the direct (luminance change) condition, in which the luminance of the central patch that covers the receptive field of the neuron is varied sinusoidally in time at 0.5, 1, 2, and 4 Hz, and (b) the simultaneous contrast condition, in which the luminance of flanking patches is varied sinusoidally in time at 0.5, 1, 2, and 4 Hz, which would typically induce a simultaneous contrast effect in humans.

Rossi and Paradiso (1999) discovered that: (a) it is not uncommon for neurons to respond to the fluctuation of luminance in the direct condition, in which a uniform luminance patch covers the whole receptive field; (b) many neurons respond to the luminance fluctuation of the flankers in the simultaneous contrast condition as well (a typical neuron and

doi: 10.1167/13.1.8 Received July 13, 2012; published January 4, 2013 ISSN 1534-7362

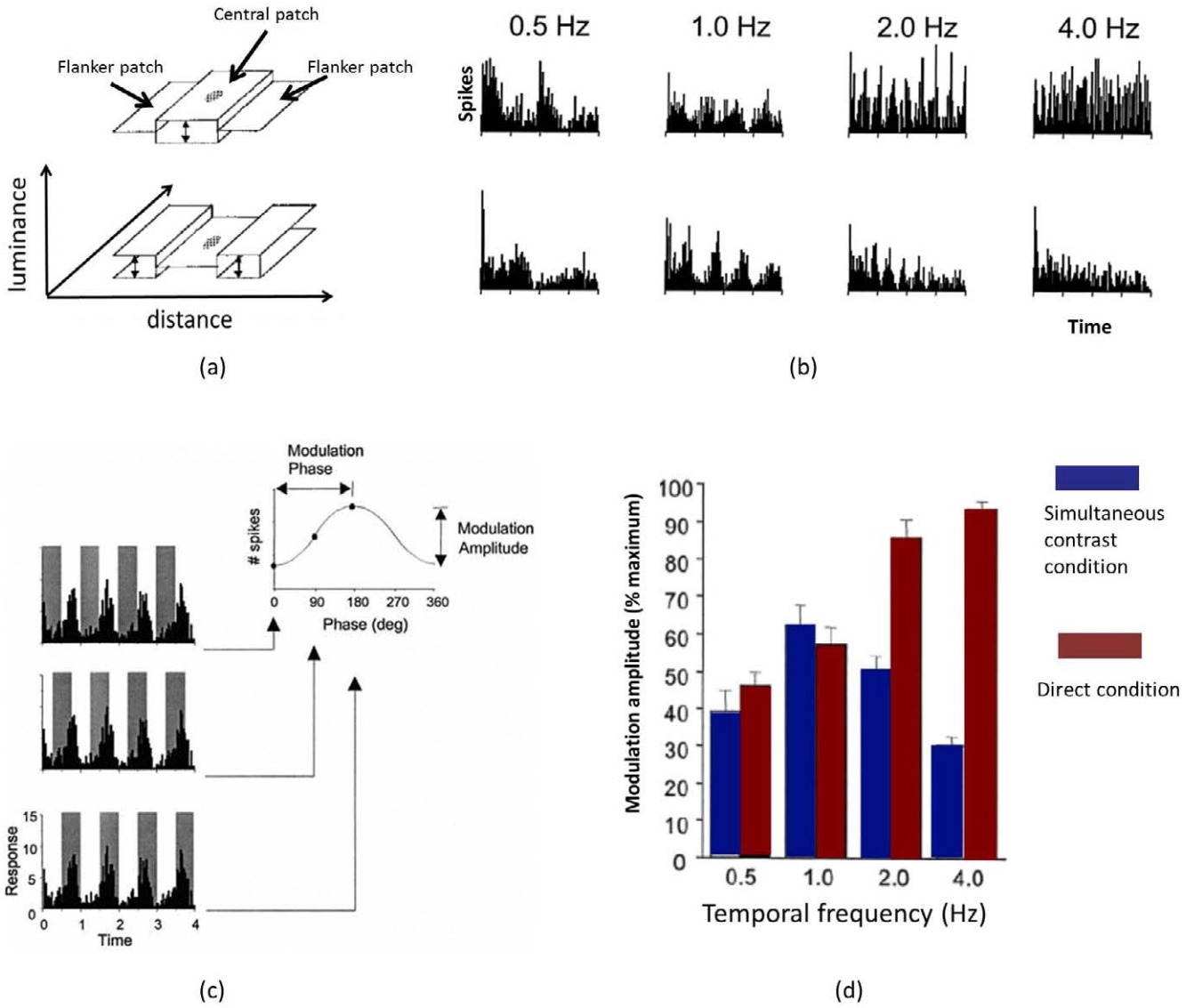

Figure 1. Modulation of brightness-related responses in two experiment conditions. (a) The direct condition (top) and simultaneous contrast condition (bottom). The central luminance patch is usually 14° × 14° in visual angle. The small spotted patch in the center represents the classical receptive field of a sampled neuron, which is usually less than 5° × 5° in visual angle. The small vertical two-sided arrows indicate the temporally fluctuating part in each condition. (b) A neuron in striate cortex that responds to luminance modulation corresponding to the conditions in (a) on the left. The receptive field of this neuron is 4° wide and 3.5° high. The responses in both conditions show a modulation by the luminance. The modulation amplitude in the direct condition (top) increases as luminance frequency increases. The modulation amplitude in the simultaneous contrast condition (bottom) decreases as luminance frequency increases over 1 Hz. (c) Schematic illustration of the procedure used to quantify the degree of modulation in the response histogram. On the left of the figure is the response of a neuron to the induction stimulus at a luminance modulation rate of 1 Hz. To assess the degree of modulation in the poststimulus time histogram (PSTH), the neural response is multiplied by a sliding square wave weighting function having a period equal to the inverse of the modulation rate. The gray bands superimposed on the PSTH represent the weighting function in which the activity within the gray zones is summed. A plot of response modulation is constructed (top right) by incrementally shifting the weighting function across 360° of initial phase (left). The amplitude and phase of the response modulation sinusoid is then used to define the modulation amplitude and phase. (d) Averaged normalized modulation amplitudes for 24 striate neurons plotted as a function of the rate of luminance modulation. The modulation amplitude is expressed as the percentage of the maximum response amplitude elicited by either stimulus for each neuron. Red bars represent the response to the direct condition, and blue bars represent the response to the simultaneous contrast condition. Error bars are equal to one standard error of the mean. Adapted from Rossi and Paradiso (1999).

its response is shown in Figure 1b); and (c) the modulation amplitude (calculated as the amplitude of the responses convolved by step pulse functions with a certain temporal frequency as shown in Figure 1c) changes differently according to temporal frequencies in different conditions. In the direct condition, the modulation amplitude increases as the temporal frequency of the central luminance fluctuation increases, while in the simultaneous contrast condition, the modulation amplitude decreases as the temporal frequency of the flanker luminance fluctuation goes beyond 1 Hz and becomes only 30% of the maximum response of the neuron at 4 Hz (Figure 1d). This "cut-off frequency" of 4 Hz is similar to the temporal limit of the perception of the simultaneous contrast effect in humans (Rossi & Paradiso, 1996).

The reason why V1 neurons are so slow to respond to simultaneous contrast stimuli is not clear. We propose three minimal neural models to investigate the possible origin of the cut-off frequency at 4 Hz in the visual system. Is it because of slow local inhibition? Is it because of a preference of extrastriate neurons, which feed back to V1 neurons, for slow stimuli? Or is it because of the conduction delays along lateral connections? Though it is possible that multiple mechanisms are responsible for the slow response of V1 neurons, we seek to capture the principal elements that contribute to the temporal pattern of the observed responses to simultaneous contrast stimuli in V1. Further experimental studies can then investigate the specific mechanisms underlying these elements.

The models

We develop and compare three models to account for the temporal modulation of V1 neuron responses to the luminance fluctuation in both the direct condition and the simultaneous contrast condition across a range of temporal frequencies (0.5 to 4 Hz) (Rossi et al., 1996; Rossi & Paradiso, 1999). The three models share the same spatial structure, as shown in Figure 2, which is similar to a two-layer Wilson-Cowan model with simplified connections (e.g., no recurrent connection for each node) as described below (Wilson & Cowan, 1973; see also Hermens, Luksys, Gerstner, Herzog, & Ernst, 2008). Each of the two layers contains a one-dimensional array of excitatory nodes (E) and inhibitory nodes (I). Each pair of E and I nodes with the same index number represents the same location in the visual field with the same receptive field center. Each E node in Layer 1 receives an excitatory input from an external signal with the same index representing the same location in the visual field, and each E node in Layer 2 receives excitatory inputs from an E node in Layer 1 with the same index and its neighbors. Each E node in any of the two layers receives an inhibitory input from an I node with the same index in the same layer. I nodes in Layer 1 receive excitatory input from E nodes in Layer 2, while I nodes in Layer 2 receive excitatory input from E nodes with the same index in Layer 2.

E nodes represent the group of excitatory neurons responding to luminance, including uniform surface luminance, which are commonly observed in V1 (Rossi et al., 1996; Rossi & Paradiso, 1999; Huang & Paradiso, 2008). I nodes represent inhibitory interneurons. We use the term "node" to refer to the modeled neuron and the term "neuron" to refer to the biological neuron in brain. The concept of nodes and connections here is much simplified compared to reality, because we intend to capture the principle factors of the slow modulation of neural responses that are related to brightness. We regard the response of the node to represent a population firing rate and do not consider the detailed biophysical properties of neurons. We also treat the connections between the nodes as representing the set of synapses between the corresponding populations. We keep the connectivity structure and parameters of the models as minimal as possible, as long as they suffice to fit the data.

An extremely simplified version of our three models would be one pair of nodes representing the location covered by the central patch and one pair representing that covered by the flanking patch in the simultaneous contrast condition in each layer. In Figure 3, only the pair representing the central patch in Layer 1 and the excitatory node representing the flanking patch in Layer 2 are shown. The nodes and the projection marked as red are considered as the main cause of the cut-off at 4 Hz of the modulation of responses to simultaneous contrast stimuli for each respective model. In the Slow Inhibition Model, this main cause is the slow inhibitory node; in the Slow Excitation Model, this main cause is the slow excitatory node in Layer 2; in the Delay Model, this main cause is the conduction delays along the lateral projections (the lateral projections can be considered as feedback or as horizontal connections, see Discussion for details).

To mimic the conditions of the Rossi and Paradiso (1999) experiment in one dimension, we set each layer to represent 42° of visual angle. In the direct condition, only the nodes representing the central patch receive input varying over time, while in the simultaneous contrast condition, only the nodes representing the flanking patch receive input varying over time. Each two adjacent nodes have a 3° gap between their receptive fields. The gap or overlap further determines the number of nodes. Because we normalize the weights of connections across the nodes that receive uniform inputs within the central patches or the flanker patches,

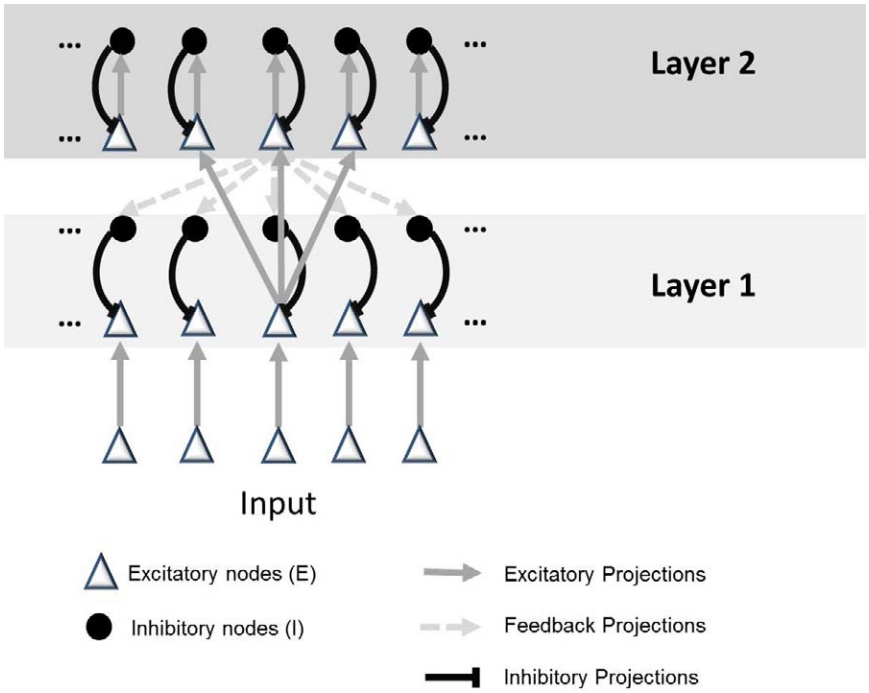

Figure 2. Connection structure of the models. Only five nodes of each layer are shown. The triangle and circle represent excitatory (E) and inhibitory (I) nodes, respectively. The projections from I nodes to E nodes are local, but the projections from E nodes of Layer 2 (E_2) to I nodes in Layer 1 (I_1) are global (see text for details).

the number of nodes does not affect the stability of the models and is not important for the results.

Layer 1 and Layer 2 have similar patterns of connections, except that: (a) each E_2 node receives projections from a pool of adjacent E_1 nodes (three by default) and thus inherits the receptive field center of the central projecting V1 node, but has a larger receptive field; and (b) each E_2 node projects to all the inhibitory nodes in Layer 1, I_1, and to the corresponding local inhibitory node in Layer 2, I_2.

The input to Layer 1 is simulated as a mean of lateral geniculate nucleus (LGN) signals activated by a region in the visual field. In other words, the input to each E_1 node is just an excitatory projection whenever the corresponding part of the visual field (one degree by default) is covered by a luminance patch without any spatially antagonistic surround. The modulation of the LGN input amplitude increases, as the frequency of the luminance stimuli increases as shown in Figure 4, black bars. We fit a linear function of temporal frequencies to the LGN response in Figure 4 and use that function for the inputs to our Layer 1 E nodes under different temporal frequencies.

The models can be formulated with a system of linear ordinary differential equations:

$$\tau_{E_1}\frac{dE_1}{dt} = -E_1 - M_{EI}I_1 + input \quad (1)$$

$$\tau_{I_1}\frac{dI_1}{dt} = -I_1 + M_{IE}E_2 \quad (2)$$

$$\tau_{E_2}\frac{dE_2}{dt} = -E_2 + M_{E_2E_1}E_1 - M_{EI}I_2 \quad (3)$$

$$\tau_{I_2}\frac{dI_2}{dt} = -I_2 + E_2 \quad (4)$$

where E_1 and E_2 are the excitatory node vectors of Layer 1 and Layer 2, respectively. I_1 and I_2 are the inhibitory node vectors of Layer 1 and Layer 2, respectively. τ_{E_1}, τ_{I_1}, τ_{E_2}, and τ_{I_2} are the corresponding time constants. M_{EI} is the connection matrix from I to E. It is a diagonal matrix, representing the local inhibition from each I node to the corresponding E node with the same index. M_{IE} is the connection matrix from E to I, with all elements having the same value, representing both local and long-range excitation to inhibitory nodes. The value of each entry is 1 / (number of E nodes) in the corresponding layer. $M_{E_2E_1}$ is the connection matrix from E_1 to E_2, representing a projection from Layer 1 nodes to Layer 2 excitatory nodes.

The Slow Inhibition Model

For the Slow Inhibition Model we consider that all the local inhibitory nodes respond slowly to the

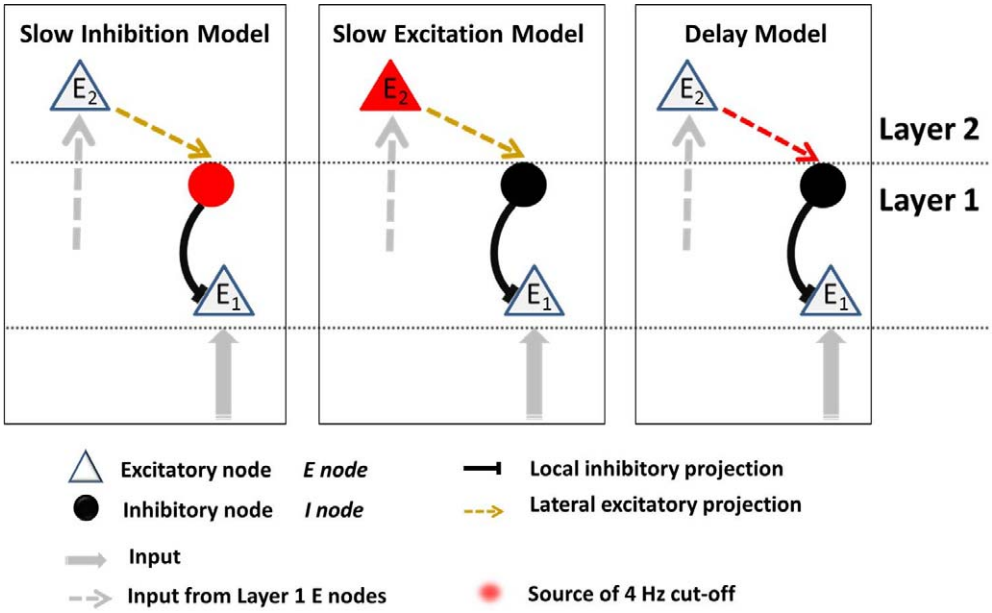

Figure 3. A summary of the three models. Left, the Slow Inhibition Model. Red color marks the main cause of the cut-off at 4 Hz in response to simultaneous contrast stimuli, which is the slow inhibitory node in this model. E_2 represents the excitatory node in Layer 2 that receives input from a Layer 1 excitatory node (not shown) corresponding to the flanker patches. E_1 represents the excitatory node receiving input corresponding to the central patch. The black disk represents the corresponding local inhibitory nodes of node E_2. Middle, the Slow Excitation Model. The main cause of the cut-off at 4 Hz is the slow excitatory node in Layer 2, marked in red. Right, the Delay Model. The main cause is the conduction delays along the lateral projections.

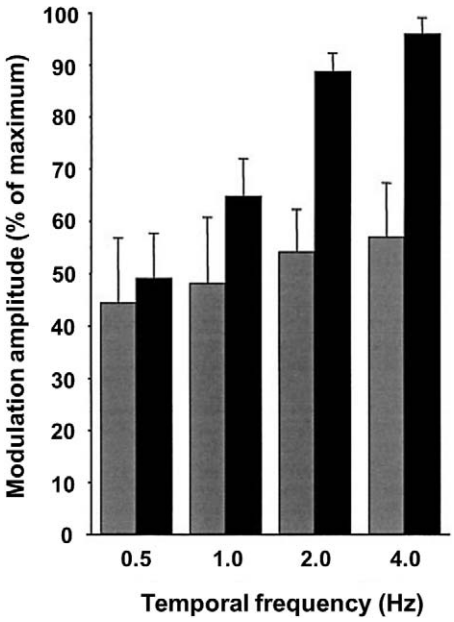

Figure 4. The mean modulation of LGN signals activated by a region in visual field. Gray bars represent the response modulation in the simultaneous contrast condition, and black bars represent the response modulation in the direct condition. The modulation amplitude is expressed as the percentage of the maximum response amplitude elicited by either stimulus for each neuron. Error bars are equal to 1 standard error of the mean. Adapted from Rossi and Paradiso (1999).

excitatory signal from Layer 2. This causes the suppression induced by the flanker luminance changes to only affect the response of the central nodes at a slow pace, and thus the modulation of the response of the central nodes starts to drop off when the luminance of the flankers fluctuates at more than a certain temporal frequency (1 Hz in the experimental data). We set $\tau_{E_1} = \tau_{E_2} = 20$ ms and varied τ_{E_2} ($\tau_{I_1} = \tau_{I_2}$ in this model). We found that when $\tau_{I_1} = \tau_{I_2} = 160$ ms, the model shows the best fit to the pattern of the modulation amplitude in the experimental data.

The Slow Excitation Model

For the Slow Excitation Model we consider that the excitatory nodes in Layer 2 respond slowly to the input from Layer 1, which will further lead to a slow response of the inhibitory nodes that receive their projections. This process will result in a slow suppressive effect of the central node response in Layer 1 in the simultaneous contrast condition, and thus the modulation of its response will cut off when the luminance of the flankers fluctuates at more than certain temporal frequencies (1 to 4 Hz in the experimental data). We set $\tau_{I_1} = \tau_{I_2} = 10$ ms and $\tau_{E_1} = 20$ ms and varied τ_{E_2}. We found that when $\tau_{E_2} = 230$ ms, the model shows the best fit to the pattern of the modulation amplitude in the experimental data.

The Delay Model

We have shown that models without conduction delays but with slow responses of inhibitory nodes (the Slow Inhibition Model) and slow responses of Layer 2 excitatory nodes (the Slow Excitation Model) can be fit to the experimental data. We further investigate an alternative of the source of the slow modulation of neural responses to the induced brightness. One intuitive way is to introduce conduction delays along the connections. We will show that the Delay Model can also model the rapid response that leads to the increasing modulation amplitude under the direct condition and to a cut-off of the modulation amplitude under the simultaneous contrast condition.

Conduction delays depending on the distance between the source and target

We apply conduction delays to the feedback projections from Layer 2 to Layer 1. We set the time constant of inhibitory nodes to 10 ms and the time constant of excitatory nodes to 20 ms. The delay depends on the distance between the projection node and the target node, which is the product of the distance between their receptive field centers (degrees) and 1 mm/° (refer to Discussion section for a detailed discussion of the cortical magnification factor). The conduction speed is varied in the range of 0.01 mm/ms to 0.5 mm/ms. We will show that this type of model can also fit the data of Rossi and Paradiso (1999) at certain conduction speeds, e.g., 0.08 mm/ms, which means 12.5 ms delay per mm.

Because we are considering the response of a group of neurons for each model node, it is reasonable that not all the neurons represented by the model node have the same conduction delay to a target group of neurons. In other words, signals from neurons in one group do not necessarily reach some neurons in the target group at exactly the same time as other neurons in the same group. This means that if we randomly choose one neuron from one group and one neuron from another group, record the conduction delay between the time when the signal is sent from the projecting neuron and the time when the signal is received by the target neuron and keep doing this again and again, we will get a distribution of the conduction delays between these two groups, rather than a single value. The origin of the randomness of the delay could be due to both the transmission speed and the total distance and total number of synapses between each neuron pair from the source and target groups. However, it is very hard to experimentally measure the conduction delay distribution between two groups of neurons, each of which represents the same location in the visual field. Thus, in this model we assume Poisson distributions for the conduction delays of horizontal connections and feedback connections, because given two groups of neurons, one as the projecting group and the other as the target group, no neuron has zero delay, and without further information, we would assume the distribution peak only once at the mean, which depends on the distance between the two groups.

Results

Temporal patterns of response modulation to simultaneous contrast stimuli

The nodes in Layer 1 of our models represent a group of neurons responding to a region of uniform luminance in V1. The nodes in Layer 2 of our models represent a group of neurons in the extrastriate cortex that receive inputs from those V1 neurons that respond to uniform luminance. We focus on the responses of the central node in the three models, because the data that these models address are obtained from neurons whose CRFs were centered with respect to the stimulus display. We first simulate the responses of the central node under three conditions: (a) uniform luminance of 42°; (b) the direct condition, in which only the central patch (14°) changes its luminance sinusoidally in time, while the luminance of the flanker patches (14°) is held to a small but nonzero constant value; and (c) the simultaneous contrast condition, in which only the flanker patches (14°) change their luminance sinusoidally in time, while the luminance of the central patch (14°) is held to the median value of the flanker luminance range.

In order to show the modulation amplitude patterns under different conditions, we use a similar technique as used in Rossi et al. (1996) and Rossi and Paradiso (1999) for the direct and simultaneous contrast condition (Figure 1c). We convolve the temporal response of the central node with a sinusoidal function having the same temporal frequency as that of the luminance change in the central (flanker) part of the stimuli in the direct (simultaneous contrast) condition. We then change the phase of the sinusoidal function in 45° steps and obtain a plot of convolved activity as a function of temporal phase of luminance. The modulation amplitude is the difference between the maximum and minimum of this phase plot, and the modulation phase is the phase of this plot, which is the phase difference between the phase of response modulation and the phase of the luminance change in the stimuli. Figure 5 shows the modulation amplitudes at a range of temporal frequencies (0.5 to 4 Hz) under the direct and simultaneous contrast conditions for

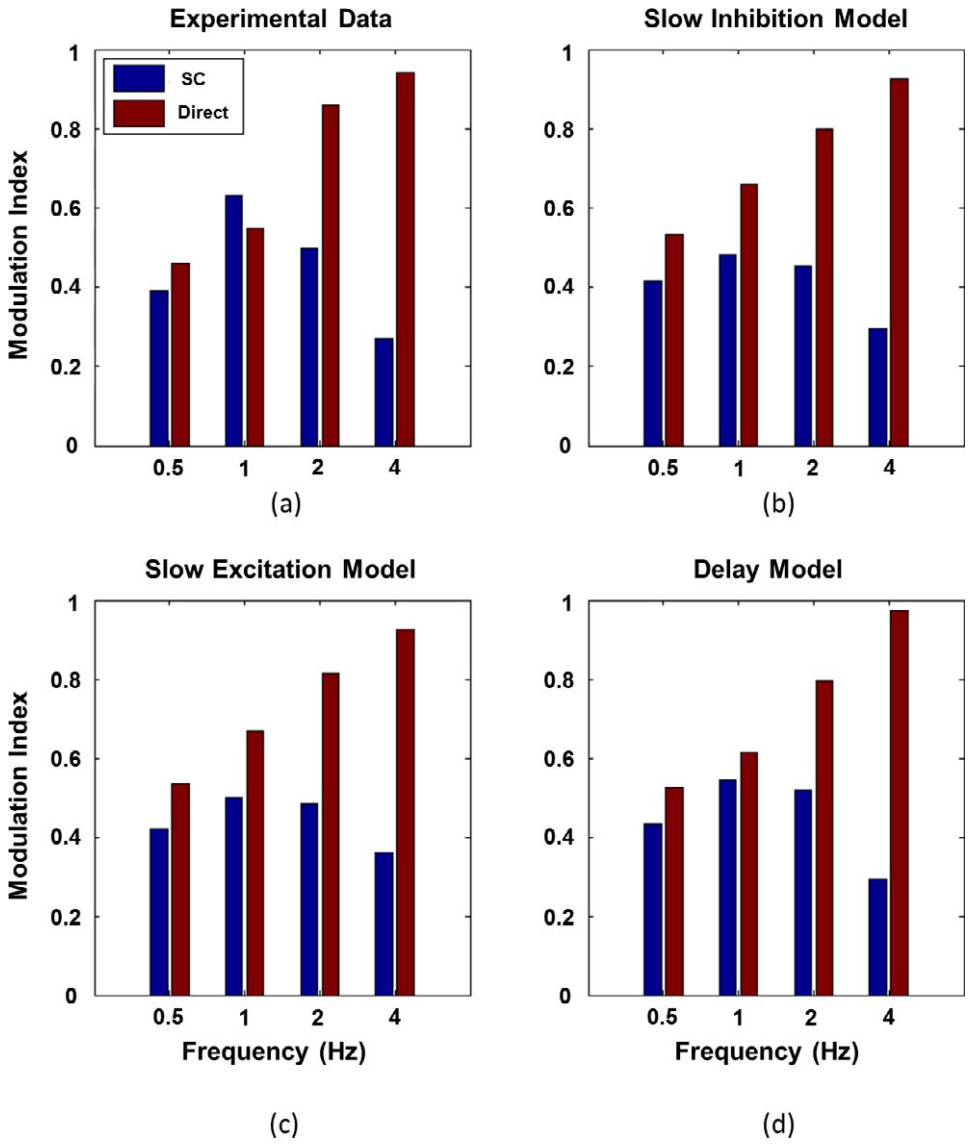

Figure 5. Modulation indices of the central nodes in Layer 1 of the three models at a range of temporal frequencies (0.5 to 4 Hz) under the direct and simultaneous contrast (SC) conditions. (a) A reproduction of experimental data with hand-marked values directly from Figure 1d. No error bar is shown here. (b) through (d) All three models can replicate the pattern of modulation in the experimental data. See the text for the details of how the index is calculated. Red bars represent the modulation index under the direct luminance condition. Blue bars represent the modulation index under the simultaneous contrast condition.

each model. The modulation amplitudes are normalized, with the maximum responses of the node across all the conditions and all the models. The maximum responses are corrected by subtracting a fixed value (0.4, maximum responses are usually slightly less than one) to obtain a value near to one for the maximum modulation amplitude. We use the normalized modulation amplitude as the modulation index to compare each model with the experimental data. A quantitative measurement of the models' fits is shown in Figure 6, which indicates a high correlation between the models' responses and the experimentally measured neural responses. All three models show a pattern of modulation similar to the experimental data, although they have different values of temporal parameters. Table 1 summarizes the temporal parameters for each model.

Phase shift property

For the simultaneous contrast condition, the central nodes in all the models show a phase shift property, which is similar to the experimental observation of cat V1 neurons that show anti-phased responses to the luminance changes of flankers in Rossi and Paradiso (1999). This means that the phase difference between the modulation phase and the phase of the flanker

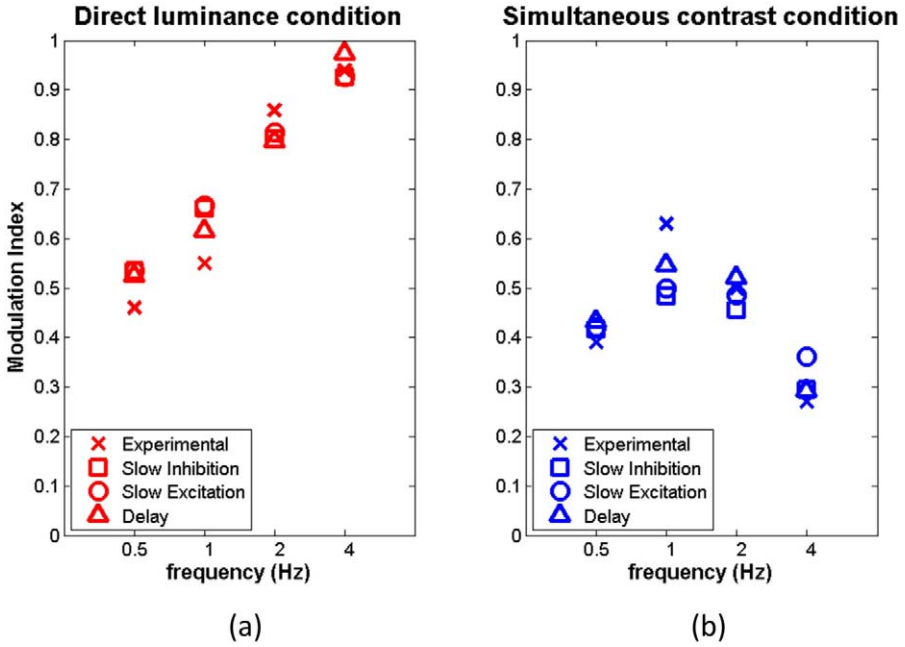

Figure 6. Model fits to the experimental data. (a) The modulation indices of the experimental data and the data of the three models in the direct condition, modified from the same data in Figure 5. The Pearson correlation coefficient between each model and the experimental data is 0.97, 0.98, and 0.97, for Slow Inhibition Model, Slow Excitation Model, and Delay Model, respectively (rounded to the nearest hundredth). (b) Similar to (a), the modulation indices of the experimental data and the data of the three models in the simultaneous contrast (SC) condition (data shown are adjusted slightly by the mean of each model). The Pearson correlation coefficient is 0.93, 0.97, and 0.95, for Slow Inhibition Model, Slow Excitation Model, and Delay Model, respectively (rounded to the nearest hundredth).

luminance change goes from 180° towards 0° as the temporal frequency of the luminance change increases, which means that the modulation phase has a tendency to shift from the opposite phase towards the phase of the flanker, as the temporal frequency of the flanker luminance change increases (Figure 7). No quantitative experimental data are currently available for comparison (Paradiso, personal communication). However, it is clear that all three mechanisms of slow modulations of responses to induced brightness in the models show a phase shift property under conditions similar to those of the experiments (e.g., increasing the temporal frequency of the flanker luminance change). We predict that the phase shift property is experimentally measurable, since it is a natural consequence of slow response modulation. In our model, the phase shift caused by slow response modulation lags behind the luminance modulation in the stimulus, which will lead to the phase difference being zero or even beyond zero as the luminance changes faster than 4 Hz (see the result of the Delay Model in 4 Hz in Figure 7 for an example).

Responses of nodes other than the central node in Layer 1

Although the central node in Layer 1 shows response modulation in both direct luminance and simultaneous contrast conditions, similar to the neurons in cat V1, other nodes in Layer 1 and Layer 2 show different responses. For the Slow Inhibition Model, the central node in Layer 2 shows a response modulation drop after 4 Hz in the simultaneous contrast condition, but it shows increasing modulation in the direct luminance condition (Figure 8, left). This characteristic implies that if the response modulation is due to the slow local inhibition in an area beyond V1, such as V2, then neurons will also show response modulation that drops at 4 Hz in the simultaneous contrast condition, but they will show increasing response modulation as the temporal frequencies of luminance changes increases in the direct luminance condition. For the Slow Excitation Model, Layer 2 nodes show slow response modulation in both

Models	τ_{E1}	τ_{E2}	τ_{I1}	τ_{I2}	Conduction delay
Slow Inhibition	20 ms	20 ms	160 ms	160 ms	1 ms
Slow Excitation	20 ms	230 ms	10 ms	10 ms	1 ms
Delay	20 ms	20 ms	10 ms	10 ms	Distance dependent 12.5 ms/mm

Table 1. Summary of parameters in the three models

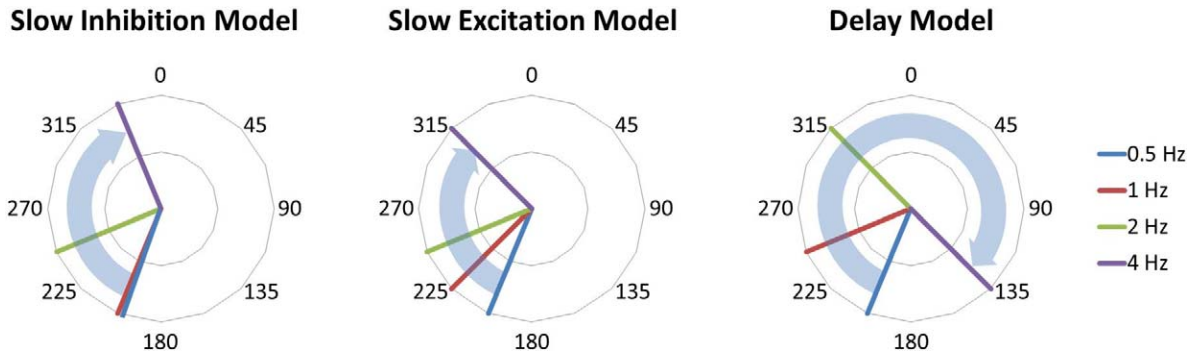

Figure 7. The phase shift property. For the simultaneous contrast condition, all the models show a phase shift property, which means that the difference between the modulation phase and the phase of the flanker luminance change goes from 180° towards 0° as the temporal frequency of the flanker luminance change increases (for the Delay Model, this difference goes over 0°). That is to say the antiphased modulation is reliable at 0.5 and 1 Hz as shown in each plots, and the modulation phase has a tendency to shift towards the phase of the flanker as the temporal frequency of the flanker luminance change increases. This is consistent with the experimental observation (Rossi & Paradiso, 1999). See Figure 1c for how the phase difference is calculated.

conditions, which means that Layer 2 nodes cannot even follow the direct luminance at 4 Hz, and cut off at 8 Hz (Figure 8, center). Thus, the Slow Excitation Model predicts that in an area beyond V1, such as V2, neurons have a preference for slow stimuli for both conditions. For the Delay Model, the central node in Layer 2 shows a cut-off frequency at 4 Hz of response modulation for simultaneous contrast conditions, but it shows increasing modulation in the direct luminance condition (Figure 8, right). In addition, the response modulation of nodes in Layer 1 in the simultaneous contrast condition depends on their locations, since the delay depends on the distance. Thus, the Delay Model predicts that within V1, the response modulation can be different according to the CRF location of the probed neuron relative to the stimuli in simultaneous contrast condition. None of these predictions have been tested experimentally to date.

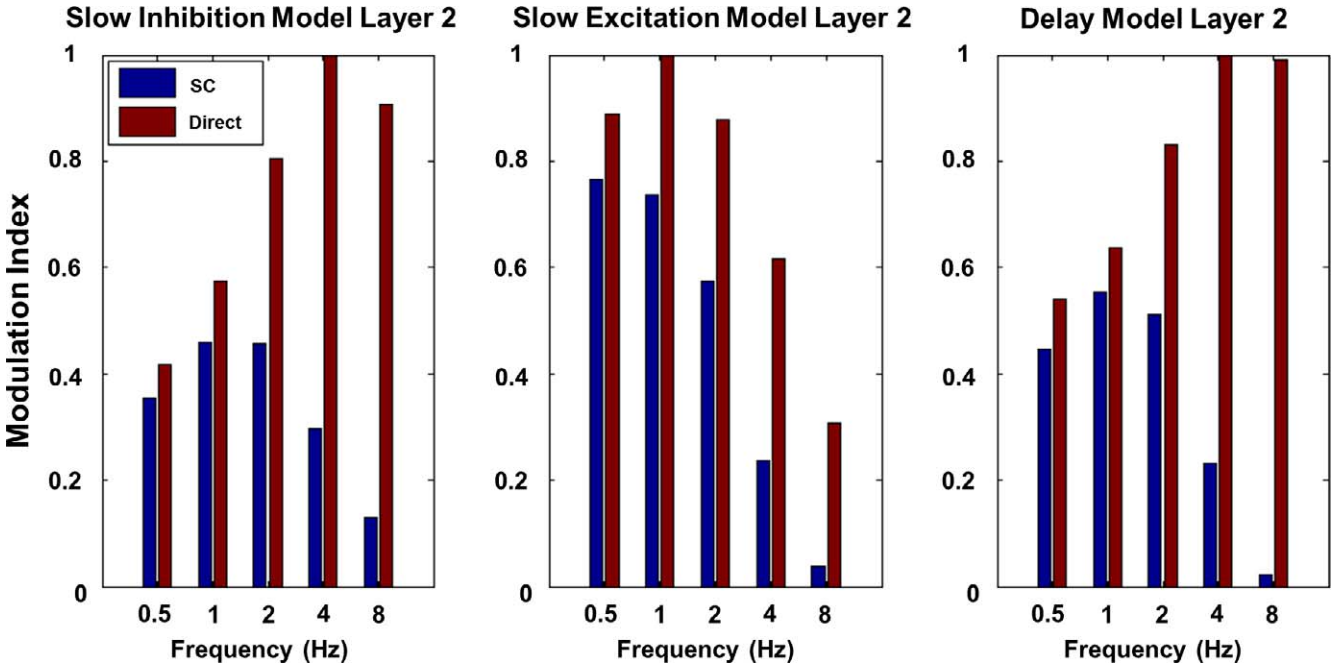

Figure 8. Modulation indices of the central nodes in Layer 2 of the three models at a range of temporal frequencies (0.5 to 8 Hz) under the direct and simultaneous contrast (SC) conditions. Left and right: the central nodes of the Slow Inhibition Model and the Delay Model both show a cut-off frequency at 4 Hz in the SC condition. They can follow the flanker luminance change in the direct condition. Center: the Slow Excitation Model generally shows a decrease of response modulation for both conditions. Red bars represent the modulation index under the direct luminance condition. Blue bars represent the modulation index under the simultaneous contrast condition.

Discussion

Previous experimental studies have reported that V1 neurons can respond to a region of uniform luminance (Kinoshita & Komatsu, 2001; Friedman et al., 2003; Roe et al., 2005). Some V1 neurons even show responses modulated by the luminance change of surrounding areas, or flankers that are several degrees away from the their CRFs, while the luminance of the area that covers their CRFs stays constant (Rossi et al., 1996; Rossi & Paradiso, 1999). Some of these neurons show responses that are antiphase to the luminance change of flankers, but show responses in-phase to direct luminance change. These responses are consistent with the human perception of brightness. The modulation of these neurons' responses to the simultaneous contrast stimuli cut off at 4 Hz, while the modulation of their responses to direct luminance increases with temporal frequency of the luminance change, which is also consistent to the result shown in human psychophysical studies (Valois, Webster, Valois, & Lingelbach, 1986; Rossi & Paradiso, 1996). Our models in this study, with only two to three temporal variables, successfully fit several properties of the experimental data, including the cut-off frequency of the response modulation by flankers at 4 Hz in the simultaneous contrast condition, the increasing modulation of responses in the direct luminance condition, and the phase shift property of neural responses in the simultaneous contrast condition (Rossi et al., 1996; Rossi & Paradiso, 1999). These three models have similar spatial layouts of nodes and connections and differ from each other by their temporal properties. The Slow Inhibition Model can fit the data mainly because of the slow local inhibitory nodes in both layers. It predicts that neurons in extrastriate cortex show fast response modulations to both direct luminance and simultaneous contrast stimuli without further feedback signals. The Slow Excitation Model can fit the data mainly because of the slow excitatory nodes in the second of two layers, which feed back to the inhibitory nodes in the first layer. It predicts that neurons in extrastriate cortex show slow modulations of the responses to both the direct luminance change and the simultaneous contrast stimuli, which is different from the modulations of V1 neurons shown in the experimental data. The Delay Model predicts that the cut-off frequency of response modulation depends on the distance from the flanker to the CRFs of the neurons.

Suppression as the main effect

Both the brightness-related responses of V1 neurons and the human perception induced by the simultaneous contrast stimuli are mainly suppressive effects (Rossi & Paradiso, 1996, 1999). To be specific, when the luminance of the flanker is lower than the central luminance patch, there is limited, if any, facilitation to the strength of the perceived brightness for human subjects, as well as to the responses of those brightness (antiphased) neurons. When the luminance of the flanker is higher than the central luminance patch, there is significant suppression to the strength of the perceived brightness for human subjects as well as to the responses of those (antiphased) neurons responding to such conditions. Our models use the inhibition induced by inputs from a long distance to achieve the suppression.

We focus on the temporal aspect of the brightness-related responses of V1 neurons so that we can achieve abstract but essential principles of the slow processing of brightness and the cortical mechanisms underlying this processing. However, we also realize that how our visual systems achieve such long-range suppression is not a trivial question, because most long-range connections, including intra-areal long-range horizontal connections and interareal feedback connections, are believed to be from excitatory neurons to excitatory neurons (Ts'o, Gilbert, & Wiesel, 1986; Rockland, 1997, but see also Anderson & Martin, 2009), although both human psycophysical and animal physiological studies have shown numerous cases of suppressive effect over a large visual angle (Bair, Cavanaugh, & Movshon, 2003; Petrov, Carandini, & McKee, 2005, but see also Bringuier, Chavane, Glaeser, & Fregnac, 1999). Since these long-range connections usually modulate the response of the target neuron rather than drive it directly (Kapadia, Westheimer, & Gilbert, 2000; Angelucci & Bullier, 2003), a further question would be what is the neural mechanism for the long-range modulatory effect that depends on both the current activity state of the neuron and the context outside its CRF? Moreover, how does this modulatory effect take place in a stable recurrent network, in which both local excitation and inhibition are very strong? The answers to these questions are important for understanding the cortical mechanisms of contextual effects and other general functionality of our visual systems. Computational investigations of these questions will be conducted in our future work.

Local origin of the slow process of the brightness-related response

Both the Slow Inhibition Model and the Slow Excitation Model can fit the experimental data well because of a local slow component. The main difference between their slow components is as indicated in their names: The slow component of the Slow Inhibition

Model is represented in the local inhibition in Layer 1, while the slow component of the Slow Excitation Model is represented in the local excitation in Layer 2. The Slow Inhibition Model predicts similar temporal properties of both the primary visual cortex and extrastriate cortex for the direct luminance condition and simultaneous contrast condition. That is, the pattern of the modulation amplitude against the temporal frequency of the stimuli will be similar between the primary visual cortex and extrastriate cortex for the direct luminance condition as well as the simultaneous contrast condition. To be specific, when neurons in the primary visual cortex show a cut-off frequency at 4 Hz in the simultaneous contrast condition, neurons in extrastriate cortex will show a cut-off frequency at 4 Hz as well, as long as neurons from both areas have similar temporal constants. On the other hand, the Slow Excitation Model shows a mechanism where neurons in higher levels of the visual systems tend to be activated more slowly than neurons in lower levels, meaning that the preferred temporal frequency of the stimuli, no matter whether it is direct luminance or simultaneous contrast stimuli, is lower for neurons in higher levels than neurons in the primary visual cortex. This slow component in extrastriate cortex will lead to low cut-off frequencies for both the direct condition and the simultaneous contrast condition. Neither of these two mechanisms has been tested experimentally (but see Keysers, Xiao, Földiák, & Perrett, 2001).

The physiological source of the large time constants used in the local components in the Slow Inhibition Model and the Slow Excitation Model can be from the synapses, because the property of the node in the model represents the property of a group of neurons. *GABA* receptors, especially $GABA_B$, can possibly play a role in the slow and long-lasting local inhibition (Connors, Malenka, & Silva, 1988; Tamas, Lörincz, Simon, & Szabadics, 2003; Perez-Garci, Gassmann, Bettler, & Larkum, 2006). The processing delay from multiple synaptic connections can also play a role. Our simulations show that by stacking a series of nodes with small time constants, the output can show a sluggish temporal profile, as if the output is from a node with a large time constant, sometimes even much larger than the linear sum of all the time constants of the nodes in the series, depending how we wire the nodes (see also Grossberg & Somers, 1991 for models with slow inhibition and different coupling configurations).

Quantitative analysis of intra-areal horizontal connections

Is the monosynaptic intra-areal horizontal connection alone sufficient to account for the modulation of V1 responses induced by simultaneous contrast stimuli? Anatomically, the monosynaptic horizontal connection in cat primary visual cortex can extend about 3 to 4 mm radially (Gilbert & Wiesel, 1979, 1989; Martin & Whitteridge, 1984; Hirsch & Gilbert, 1991). For the large simultaneous contrast stimuli (Rossi et al., 1996; Rossi & Paradiso, 1999), the span of the cortical distance representing the spatial extent of the stimuli can be estimated by a sample of flattened cat V1 (Tusa, Palmer, & Rosenquist, 1978) as shown in Figure 9. We are interested in the cortical distance from neurons whose receptive field centers are within the flanker patch (the flanker neurons) to the probed neuron whose receptive field is at the center of the central patch (the probed neuron). The shortest possible cortical distance from a flanker neuron to the probed neuron is the distance from the flanker neuron representing the region adjacent to the boundary of the central and flanker patches to the probed neuron. This shortest distance represents 7° of visual angle from the fovea (half of the central patch width) along the horizontal meridian, which is about 6 mm in the sample cat V1, and is larger than 3 to 4 mm. The largest possible cortical distance from a flanker neuron to the probed neuron is from the flanker neuron representing the region adjacent to the outer boundary of the flanker patch to the probed neuron. It is the cortical distance representing 21° in visual angle (half of the whole stimulus width) along the horizontal meridian, which is about 13 mm in the sample cat V1. Thus, according to this sample of a cat flattened V1, the cortical distance from a flanker neuron to a central neuron is in the range of 6 to 13 mm, which is larger than the reported length of horizontal connections (radially 3 to 4 mm).

Besides mapping the stimuli onto one sample cat V1, we further estimate the distance range from a flanker neuron to the probed neuron by using the magnification factor data, because they are obtained from multiple observations of cat V1 (Tusa et al., 1978). First, we measure the representative values of the areal magnification factor data (Tusa et al., 1978, figure 12), and then we fit their data with an exponential function:

$$M(x) = 5.5x^{-1.13} \quad (5)$$

where M is the areal magnification factor, and x is the eccentricity along the horizontal meridian in the visual field up to 60°. The power of −1.13 we estimated here agrees exactly with another computational study of cat V1 magnification factor (Mallot, 1985). As shown in Figure 10a, we then overlap our fitting function (the red solid line) with figure 12 in Tusa et al. (1978). The fit of the exponential function is very good, although the function tends to give a larger value than the reported data near the foveal region. After obtaining the above form of the exponential function, we integrate the square root of it along the horizontal meridian to

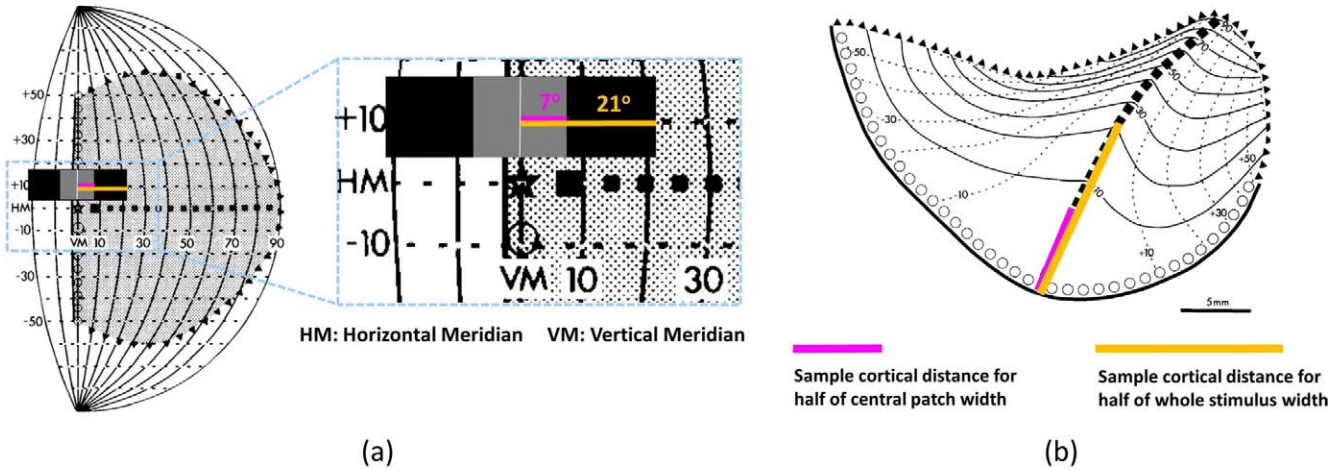

Figure 9. Mapping the simultaneous contrast stimulus to a sample of cat flattened V1. (a) Visual angles of the simultaneous contrast stimulus. The purple line represents half of the width of the central patch, 7°, which is also the distance from the boundary between the central and flanker patches to the center of the receptive field of the probed neuron. The orange line represents half of the width of the whole stimulus, 21°, which is also the largest distance from the flanker patch to the center of the receptive field of the probed neuron. (b) Mapping the visual field in (a) onto a sample of cat flattened V1. We can see the cortical distance according to 7° in visual angle is about 6 mm, while the cortical distance according to 21° in visual angle is about 12 mm, compared to the 5 mm scale bar. Thus, the distance from a neuron whose receptive field is within the flanker patch is larger than the length of horizontal connections as previously reported (unilaterally 3 to 4 mm, Gilbert & Wiesel, 1979, 1989). Both figures are adapted from Tusa et al., 1978.

estimate the cortical distance covering a visual angle along the horizontal meridian:

$$D(x_0) = \int_0^{x_0} \sqrt{M}\ \mathrm{d}x, \tag{6}$$

where D is the cortical distance, and x_0 is the visual angle to the foveal region along the horizontal meridian in the visual field up to 60°. We use the square root of M to convert the areal magnification factor to a one dimensional magnification factor. As shown in Figure 10b, we overlap our fitting function with the data of another study, which also estimates the cortical distance using the same data as used in Figure 10a (Olman, Ronen, Ugurbil, & Kim, 2003). The purple line along the y-axis marks the estimated cortical distance representing 6° in visual angle along the horizontal meridian, from 1° to 7° eccentricity, which is about 10 mm and is conservative compared to a

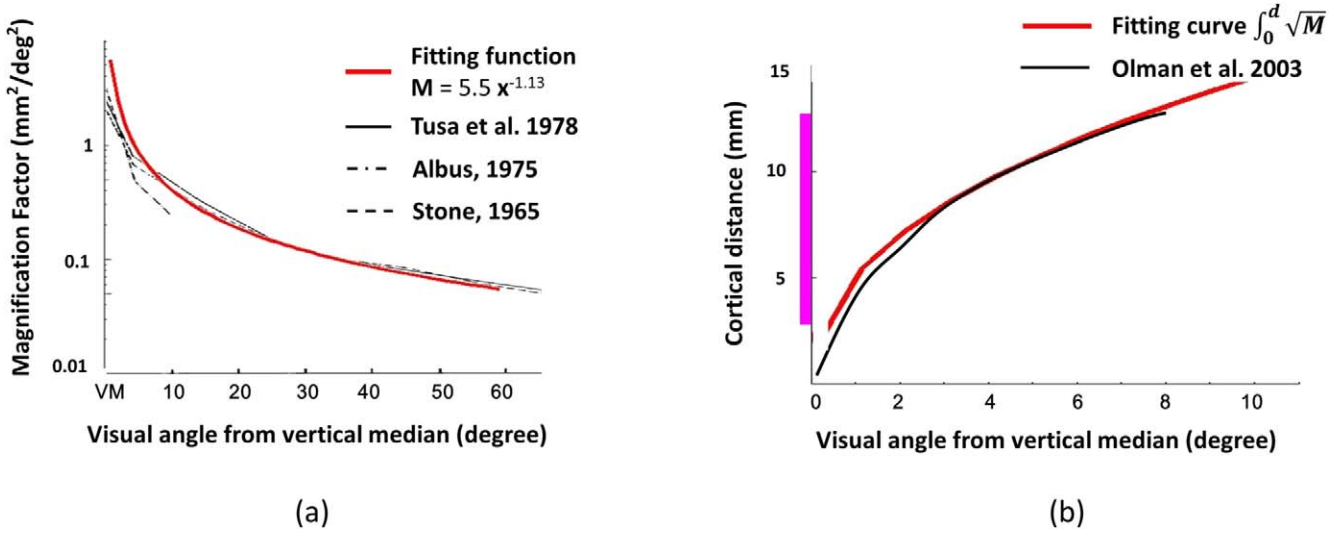

Figure 10. Fitting magnification factor and estimating the cortical distance. (a) Fitting the areal magnification factor with an exponential function (adapted from Tusa et al., 1978). (b) Estimating the cortical distance covering a visual angle from the fixation with the integral of the square root of the exponential function along horizontal meridian (adapted from Olman et al., 2003). The vertical purple line indicates the estimated cortical distance representing the visual field from 1° to 8° of eccentricity.

cortical distance covering a visual angle from 0° to 7° eccentricity. Even if we take into account the exaggerated distance estimation near the foveal region, and only consider the cortical distance representing 5° in visual angle along the horizontal meridian, from 2° to 7° eccentricity, the cortical distance is still about 5 mm, which is larger than the length of horizontal connections as previously reported (3 to 4 mm). Thus, it is unlikely that the monosynaptic horizontal connections modulate the response of foveal neurons directly.

Moreover, functional data show that cortical activities along the intra-areal horizontal connections become weaker as they travel away from the source. These cortical activities include spikes, activities measured by optical imaging, or the correlation of local field potentials (LFPs) between two displaced units (Das & Gilbert, 1995; Bringuier et al., 1999; Nauhaus, Busse, Carandini, & Ringach, 2009). For example, the correlation of LFPs can be fit by an exponential function of the distance to the source signal in the form of

$$Me^{\frac{-d}{\lambda}} \quad (7)$$

where M is the magnification factor, d is the distance to the source, and λ is a spatial constant, which represents how much the correlation drops over a unit distance. For visually driven LFPs at the source position, the spatial constant of the correlation between the source LFP and target LFP is less than 1 mm. This means that the correlation value will drop to almost one third when the target unit is 1 mm away, which is far less than the conservative result of 5 to 6 mm in the anatomical analysis. Thus, it is even more unlikely that the monosynaptic horizontal connections modulate the response of foveal neurons directly.

However, we also simulate the Delay Model with the distance calculated by the estimated function of the magnification factor (Equation 6), rather than calculated by a constant magnification factor (1 mm/°, corresponding to the magnification factor at about 2° to 3° of eccentricity) as we use in the previous sections. The conduction speed along the connection from Layer 2 E nodes to Layer 1 I nodes needs to be as slow as 0.04 mm/ms to achieve a reasonable fit (Pearson correlation: 0.92) to the modulation pattern in the physiological data (Rossi & Paradiso, 1999), which is one order of magnitude slower than the speed along horizontal connections (Hirsch & Gilbert, 1991; Bringuier et al., 1999) and two orders of magnitude slower than the speed along feedback connections (Girard, Hupé, & Bullier, 2001). This makes it less likely for the Delay Model alone to account for the slow response modulation in visual cortex in the simultaneous contrast condition.

It is also very important to apply a similar analysis to monkey studies. However, we are not aware of monkey studies that are similar to Rossi et al. (1996) and Rossi and Paradiso (1999) with respect to the stimulus size and periodic character. So we did not provide a similar analysis on monkeys in this study.

Additional considerations for the model

Our models provide three possible mechanisms to explain the slow suppressive effect induced by luminance modulation outside the classical receptive field of V1 neurons. The nodes in our models can be regarded as the group of neurons responding to luminance levels, as well as luminance changes (regardless the sign of the change). We do not distinguish these two conditions, because the luminance used in the experiment (Rossi et al., 1996; Rossi & Paradiso, 1999) and similarly our input used in this study are sinusoidal over time, the temporal derivative of which are still sinusoidal with only a phase difference. However, it is more likely that neurons modulating the tested neuron in the experiment are sensitive to luminance levels rather than luminance changes, because the latter predicts the most modulation when the flanker luminance reaches its maximum, while the former predicts zero modulation.

Although it seems possible to consider that the two layers of each model correspond to two different groups of neurons within V1, it is actually more reasonable to consider Layer 2 to represent areas beyond V1, given the spatial scale of its projections. The spatial scale of these projections needs to be large enough to account for the long-range suppressive effect in the simultaneous contrast condition, and this scale is larger than that of horizontal connections in cat V1.

As discussed in the previous section, due to the dilemma of the spatial scale and the conduction speed of the connections from Layer 2 to Layer 1, it is less likely that the Delay Model alone can account for the slow response modulation in visual cortex in the simultaneous contrast condition. But the Delay Model can be varied into a configuration that includes slow intralayer horizontal connections in both Layer 1 and Layer 2, and fast interlayer (inter-areal) feedback from Layer 2 to Layer 1. However, the focus of this study is to capture the principle component of slow brightness-related modulation with minimum number of parameters. The models that take into account the recurrent nature of the visual systems, multisynaptic long-range connections, supralinear local inhibition modulated by contextual information will be the focus of future studies.

Conclusion

We suggest three models that can fit the slow brightness-related response modulations (Rossi et al.,

1996; Rossi & Paradiso, 1999): (a) the Slow Inhibition Model; (b) the Slow Excitation Model; and (c) the Delay Model. In addition, these models show a phase shift property similar to cat V1 neurons, but they predict different response modulations of extrastriate neurons and V1 neurons whose CRFs are not at the center of the stimuli. These predictions can be tested in neurophysiological experiments, which may further clarify whether the mechanisms suggested by each of the three models play a role in the long-range modulation. We have discussed several factors related to the brightness-related response modulation, including the local inhibition and excitation, intra-areal monosynaptic horizontal connections and inter-areal feedback. Investigating the brightness-related responses both experimentally and computationally may shed light on how inter-areal feedback interact with the intra-areal recurrent network to make our visual system sensitive to contextual information, and thus adaptive to the environment.

Acknowledgments

Supported in part by CELEST, a National Science Foundation Science of Learning Center (NSF SMA-0835976).

Commercial relationships: none.
Corresponding author: Arash Yazdanbakhsh.
Email: yazdan@bu.edu.
Address: Center for Computational Neuroscience and Neural Technology, Program in Cognitive and Neural Systems, Boston University, Boston, MA, USA.

References

Anderson, J. C., & Martin, K. A. (2009). The synaptic connections between cortical areas V1 and V2 in macaque monkey. *Journal of Neuroscience*, *29*(36), 11283–11293.

Angelucci, A., & Bullier, J. (2003). Reaching beyond the classical receptive field of V1 neurons: Horizontal or feedback axons? *Journal of Physiology, Paris*, *97*(2–3), 141–154.

Bair, W., Cavanaugh, J. R., & Movshon, J. A. (2003). Time course and time-distance relationships for surround suppression in macaque V1 neurons. *Journal of Neuroscience*, *23*(20), 7690–7701.

Bringuier, V., Chavane, F., Glaeser, L., & Fregnac, Y. (1999). Horizontal propagation of visual activity in the synaptic integration field of area 17 neurons. *Science*, *283*(5402), 695–699.

Connors, B. W., Malenka, R. C., & Silva, L. R. (1988). Two inhibitory postsynaptic potentials, and GABAA and GABAB receptor-mediated responses in neocortex of rat and cat. *Journal of Physiology*, *406*(1), 443–468.

Das, A., & Gilbert, C. D. (1995). Long-range horizontal connections and their role in cortical reorganization revealed by optical recording of cat primary visual cortex. *Nature*, *375*(6534), 735–736.

Friedman, H. S., Zhou, H., & von der Heydt, R. (2003. May). The coding of uniform colour figures in monkey visual cortex. *Journal of Physiology*, *548*(Pt 2), 593–613.

Gilbert, C. D., & Wiesel, T. N. (1979). Morphology and intracortical projections of functionally characterised neurones in the cat visual cortex. *Nature*, *280,* 120–125.

Gilbert, C. D., & Wiesel, T. N. (1989). Columnar specificity of intrinsic horizontal and corticocortical connections in cat visual cortex. *Journal of Neuroscience*, *9*(7), 2432–2442.

Girard, P., Hupé, J. M., & Bullier, J. (2001). Feedforward and feedback connections between areas V1 and V2 of the monkey have similar rapid conduction velocities. *Journal of Neurophysiology*, *85*(3), 1328–1331.

Grossberg, S., & Somers, D. (1991). Synchronized oscillations during cooperative feature linking in a cortical model of visual perception. *Neural Networks*, *4*(4), 453–466, doi:10.1016/0893-6080(91)90041-3.

Hermens, F., Luksys, G., Gerstner, W., Herzog, M. H., & Ernst, U. (2008. January). Modeling spatial and temporal aspects of visual backward masking. *Psychological Review*, *115*(1), 83–100, doi:10.1037/0033-295X.115.1.83.

Hirsch, J. A., & Gilbert, C. D. (1991). Synaptic physiology of horizontal connections in the cat's visual cortex. *Journal of Neuroscience*, *11*(6), 1800–1809.

Huang, X., & Paradiso, M. A. (2008). V1 response timing and surface filling-in. *Journal of Neurophysiology*, *100*(1), 539–547.

Kapadia, M. K., Westheimer, G., & Gilbert, C. D. (2000). Spatial distribution of contextual interactions in primary visual cortex and in visual perception. *Journal of Neurophysiology*, *84*(4), 2048–2062.

Keysers, C., Xiao, D. K., Földiák, P., & Perrett, D. I.

(2001). The speed of sight. *Journal of Cognitive Neuroscience*, *13*(1), 90–101.

Kinoshita, M., & Komatsu, H. (2001). Neural representation of the luminance and brightness of a uniform surface in the macaque primary visual cortex. *Journal of Neurophysiology*, *86*(5), 2559–2570.

Mallot, H. (1985). An overall description of retinotopic mapping in the cat's visual cortex areas 17, 18, and 19. *Biological Cybernetics*, *52*(1), 45–51.

Martin, K. A., & Whitteridge, D. (1984). Form, function and intracortical projections of spiny neurones in the striate visual cortex of the cat. *Journal of Physiology*, *353*(1), 463–504.

Nauhaus, I., Busse, L., Carandini, M., & Ringach, D. L. (2009). Stimulus contrast modulates functional connectivity in visual cortex. *Nature Neuroscience*, *12*(1), 70–76, doi:10.1038/nn.2232.

Olman, C., Ronen, I., Ugurbil, K., & Kim, D.-S. (2003). Retinotopic mapping in cat visual cortex using high-field functional magnetic resonance imaging. *Journal of Neuroscience Methods*, *131*(1–2), 161–170, doi:10.1016/j.jneumeth.2003.08.009.

Perez-Garci, E., Gassmann, M., Bettler, B., & Larkum, M. E. (2006). The GABAB1b isoform mediates long-lasting inhibition of dendritic Ca2+ spikes in layer 5 somatosensory pyramidal neurons. *Neuron*, *50*(4), 603–616, doi:10.1016/j.neuron.2006.04.019.

Petrov, Y., Carandini, M., & McKee, S. (2005). Two distinct mechanisms of suppression in human vision. *Journal of Neuroscience*, *25*(38), 8704–8707, doi:10.1523/JNEUROSCI.2871-05.2005.

Rockland, K. S. (1997). Elements of cortical architecture. *Extrastriate Cortex in Primates*, *12*(1), 243–292.

Roe, A. W., Lu, H. D., & Hung, C. P. (2005). Cortical processing of a brightness illusion. *Proceedings of the National Academy of Sciences USA*, *102*(10), 3869–3874.

Rossi, A. F., & Paradiso, M. A. (1996). Temporal limits of brightness induction and mechanisms of brightness perception. *Vision Research*, *36*(10), 1391–1398.

Rossi, A. F., & Paradiso, M. A. (1999). Neural correlates of perceived brightness in the retina, lateral geniculate nucleus, and striate cortex. *Journal of Neuroscience*, *19*(14), 6145–6156.

Rossi, A. F., Rittenhouse, C. D., & Paradiso, M. A. (1996). The representation of brightness in primary visual cortex. *Science*, *273*(5278), 1104–1107.

Tamas, G., & Lörincz, A., Simon, A., & Szabadics, J. (2003). Identified sources and targets of slow inhibition in the neocortex. *Science*, *299*(5614), 1902–1905, doi:10.1126/science.1082053.

Ts'o, D. Y., Gilbert, C. D., & Wiesel, T. N. (1986). Relationships between horizontal interactions and functional architecture in cat striate cortex as revealed by cross-correlation analysis. *Journal of Neuroscience*, *6*(4), 1160–1170.

Tusa, R. J., Palmer, L. A., & Rosenquist, A. C. (1978). The retinotopic organization of area 17 (striate cortex) in the cat. *Journal of Comparative Neurology*, *177*(2), 213–235, doi:10.1002/cne.901770204.

Valois, R. L. D., Webster, M. A., Valois, K. K. D., & Lingelbach, B. (1986). Temporal properties of brightness and color induction. *Vision Research*, *26*(6), 887–897, doi:10.1016/0042-6989(86)90147-1.

Wilson, H. R., & Cowan, J. D. (1973). A mathematical theory of the functional dynamics of cortical and thalamic nervous tissue. *Kybernetik*, *13*(2), 55–80.